CONCENTRATION AND CHEMICAL COMPOSITION OF $PM_{2.5}$ AND $PM_{10\text{-}2.5}$ IN THE NORTHEASTERN MEDITERRANEAN

NILGÜN KUBILAY*
Institute of Marine Sciences-Middle East Technical University,
P.O. Box 28, Erdemli-Mersin 33731, Turkey
MUSTAFA KOÇAK
Institute of Marine Sciences-Middle East Technical University,
P.O. Box 28, Erdemli-Mersin 33731, Turkey
NIKOS MIHALOPOULOS
Environmental Chemical Process Laboratory, Depart. Of Chemistry,
University of Crete, P.O. Box 2208, Gr-71003 Voutes, Heraklion, Greece

Key Words: $PM_{2.5}$; PM_{10}; air quality; Saharan dust; eastern Mediterranean; Turkey.

Abstract Two stage aerosol samples ($PM_{10–2.5}$ and $PM_{2.5}$) were collected at a rural site (Erdemli) located on the coast of the Northeastern Mediterranean, between April 2001 and April 2002. A total of 581 aerosol samples were analysed for trace elements (Fe, Ti, Mn, Ca, V, Ni, Zn, Cr) and water soluble ions (Na^+, NH_4^+, K^+, Mg^{2+}, Ca^{2+}, Cl^-, Br^-, NO_3^-, SO_4^{2-}, $C_2O_4^{2-}$ and MS^-). The annual mean PM_{10} and $PM_{2.5}$ levels were 36.4 ± 27.8 μg m^{-3} and 9.7 ± 5.9, respectively. The highest levels of PM_{10} were observed during the transition period (March, April and May) due to mineral dust transported from North Africa and during winter due to sea spray generation. However, $PM_{2.5}$ levels exhibited higher concentrations during summer resulting from an enhanced production of secondary aerosols. PM_{10}, crustal elements, sea salt aerosols and NO_3^- were mainly associated with the coarse mode whereas $nssSO_4^{2-}$, $C_2O_4^{2-}$, MS^-, NH_4^+, Cr and Ni were found predominantly in the fine fraction. Ionic balance analysis performed in the coarse and fine aerosol fractions indicated anion and cation deficiency due to CO_3^{2-} and H^+, respectively. A relationship between $nssSO_4^{2-}$ and NH_4^+ denoted that sulphate particles were partially neutralized (70%) by ammonium. Excess-K/BC presented two distinct ratios for winter and summer, indicating two different sources: Fossil fuel burning in winter and biomass burning in summer.

1. Introduction

Aerosols physically affect the heat balance of the Earth, both directly by reflecting and absorbing solar radiation, and by absorbing and emitting

A. Mellouki and A.R. Ravishankara (eds.), Regional Climate Variability and its Impacts in the Mediterranean Area, 167–180.

some terrestrial infrared radiation and indirectly by influencing the properties and cloud processes and, possibly, by changing the heterogeneous chemistry of reactive greenhouse gases (e.g., O_3; IPCC, 2001 and references therein). The global radiative forcing due to aerosols is roughly 1.6 ± 1.3 Wm^{-2}, which nearly compensates for the mean global radiative forcing of 2.4 ± 0.3 Wm^{-2} due to greenhouse gases warming. Recently, Vrekoussis et al., (2005) investigated aerosol optical properties in the Eastern Mediterranean and estimated radiative forcing at the top of the atmosphere ranging from –12.6 to –2.3 W m^2 for summer and winter, respectively. Their estimated radiative forcing values are up to five times higher than that induced by greenhouse gases but opposite in sign. The large range of uncertainty associated with aerosol forcing estimates reflects the poor state of knowledge regarding the sources, distributions, and properties of atmospheric aerosols.

The need for an increased effort in characterizing tropospheric aerosols in order to reduce the uncertainty in the aerosol forcing estimate has been stressed (Ramanathan et al., 2001; Kaufman et al., 2002). Recent model studies reproduced satellite observations and demonstrated the role of three major components of aerosols in surrounding regions of the Mediterranean basin (sulfate, black carbon and dust), having very high direct radiative forcing for aerosols at the top of the atmosphere (Jacobson, 2001). Knowledge of the spatial and temporal variability of aerosol concentrations, their physical, chemical and radiative properties are very important since they can directly and indirectly influence planetary albedo (climate).

2. Material and Methods

A Gent type PM_{10} stacked filter unit (SFU) sampler was used in order to collect atmospheric particles in two size ranges namely, $PM_{10–2.5}$ (coarse) and $PM_{2.5}$ (fine) at a rural site located on the coast of the Eastern Mediterranean, Erdemli (36°N and 34°E), Turkey (for more details see Kubilay and Saydam, 1995; Kubilay et al., 2002; Koçak et al., 2004a, 2004b).

Sampling commenced in April 2001 and ended in April 2002. During this period a total of 562 aerosol filter samples were collected with a temporal resolution of 24 hours. After collection of aerosol filters, $PM_{10–2.5}$ and $PM_{2.5}$ concentrations were determined gravimetrically (PM_{10} refers to the sum of $PM_{10–2.5}$ and $PM_{2.5}$ concentrations). Water soluble ions were measured by ion chromatography (IC) at ECPL (Environmental Chemical Processes Laboratory), University of Crete following the method described in details by Bardouki et al. (2003). Concentrations of the elements (Fe, Ti, Ca, Mn, K, Cr, V, Zn, Cl, S) were obtained using 2 cm^2 of the filter sample applying Proton Induced X-ray Emission (PIXE) at ATOMKI (Institute of Nuclear Research of the Hungarian Academy of Sciences, Debrecen, Hungary).

During the experiments the aerosol samples were irradiated by a 2 MeV proton beam, which was supplied by the 5 MV Van de Graaff Accelerator of ATOMKI (for more details see Borbely-Kiss et al., 1999). Black Carbon (BC) content in 46 fine aerosol filter samples collected during winter and summer was determined using a Smoke Stain Reflectometer (SSR).

3. Results and Discussion

3.1. GENERAL CHARACTERISTICS OF THE DATA

The largest portion of the atmospheric particle mass (PM_{10}) is associated with coarse particles and contributes 73.4% to the observed particle mass., and the fine fraction contributes only 26.6% of the particle mass. Crust originated trace metals, water-soluble ions Na^+, Cl^-, Mg^{2+}, Ca^{2+}, Br^- and NO_3^- are associated mainly with coarse particles (more than 75%). The above observations are expected for trace metal and ions known to arise from sea salt (Na^+, Cl^-, Mg^{2+}, Br^-) and crustal material (Fe, Ti, Mn, Ca^{2+}), respectively. On average about 85% of particulate nitrate (NO_3^-) was associated with coarse particles, which would strongly indicate that it combines mostly with alkaline ion species. The most likely formation pathway for particulate nitrate (NO_3^-) is the reaction of gaseous nitric acid or some other nitrogen compounds with sea salt particles and mineral dust particles. The mass concentration of oxalate ($C_2O_4^{2-}$) and non-sea salt sulfate ($nssSO_4^{2-}$) was mainly found in the fine mode (60% and 80%, respectively). On the other hand, ammonium (NH_4^+) and methane sulfonic acid (MS^-) mass concentrations were exclusively found in the fine size fraction. Trace metals V and Zn displayed almost half of their mass concentrations in the coarse fraction while about 40% and 30% of the mass concentrations of Ni and Cr were found in coarse fraction, respectively.

Figure 1 illustrates the regression analysis between nss-SO_4^{2-} and NH_4^+ in fine aerosol particles during the observation period. The slope of the regression line is 0.68 ($NH_4^+/nssSO_4^{2-}$ equivalent ratio, r = 0.96), which indicates that partial neutralization of nss-SO_4^{2-} by NH_4^+ occurs. Taking into the account the slope of the regression, it can be proposed primarily that $(NH_4)_{1.4}.(H)_{0.6}.(SO_4)$ is produced instead of $(NH_4)_2SO_4$ in the reaction between ammonium and non sea salt sulfate.

Relationships between black carbon (BC) and other species were also investigated in 46 fine aerosol filter samples. Black carbon and excess potassium indicated strong correlation in summer and winter. Therefore, except excess potassium, BC did not indicate strong correlations with water soluble ions and elements in the dataset. Figure 2 presents the relationship between

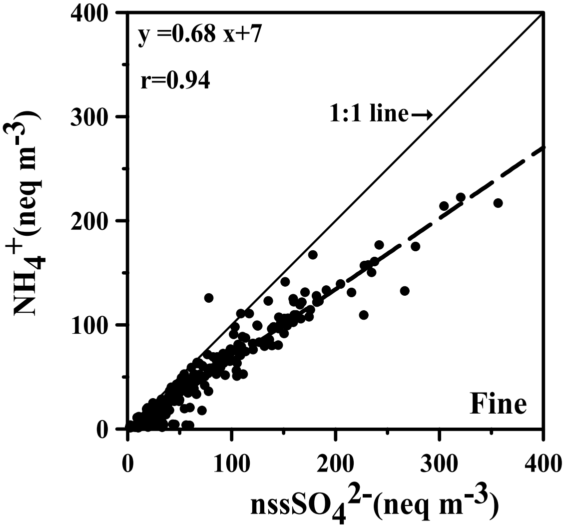

Figure 1. Observed relationship between $nssSO_4^{2-}$ and NH_4^+ (neq m^{-3})

BC and excess potassium. BC is emitted uniquely from combustion processes, including fossil fuel and biomass burning, while combustion of fossil fuel seems to produce a small amount of excess potassium. As a result, Andreae (1983) suggested that the mass ratio of excess potassium to BC may provide information enabling the distinction between the K that would be produced by biomass burning and combustion sources. As can be inferred from Figure 2 the excess potassium to BC ratio indicates two distinct ratios. The slope of the regression line in summer was found to be ~0.366 and close to the values generally measured in aerosols dominated by biomass burning (0.21 to 0.46; Andreae, 1983). Therefore, the observed ratio implies that biomass burning makes an important contribution to fine black carbon in the summer. However, the slope of the regression line in winter was about (0.062), 5 times lower than that found in summer and is similar to those found in an urban atmosphere dominated by fossil fuel burning (K/BC = 0.025-0.09, Yang et al., 2005). Hence an excess K to BC ratio suggests that fossil fuel burning predominant the source of fine black carbon particles during winter. Sciare et al., (2003) collected a total of 56 aerosol samples during summer at Finokalia (Central Mediterranean, from 26 July to 18 August 2001) and showed a nssK/BC ratio of ~0.044 (R^2 = 0.58) which was similar to the winter excess K/BC ratio observed at Erdemli. Therefore, their observed ratio suggests that potassium and BC is mainly influenced by fossil fuel burning during summer.

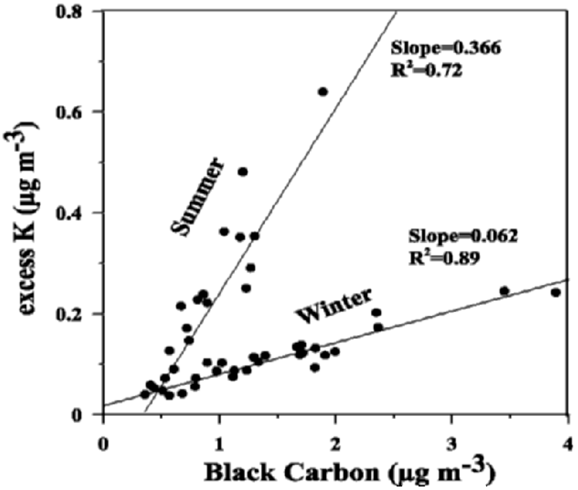

Figure 2. Relationship between excess potassium and black carbon in summer and winter

3.2. ABSOLUTE PRINCIPAL FACTOR ANALYSIS

In order to identify sources, factor analysis (FA), which is one of the multivariate statistical techniques, was carried out. Factor analysis is commonly used in environmental studies to deduce sources from data. The principal application of factor analysis is to reduce the number of variables. Therefore, factor analysis can be applied as a data reduction method. The results of varimax-rotated factor analysis are presented in Table 1a and Table 1b for atmospheric coarse and fine particles, respectively.

(A) Coarse Particles: The data can be interpreted on the basis of four common factors accounting for 87.8% of the total variance of the system. The first factor has high loadings of Ti, Fe, Mn and Ca^{2+} and moderate loadings of Zn and V. Since Factor-1 is heavily influenced by the concentrations of Ti, Fe, Mn and Ca^{2+} it may be attributed to the crustal component of the coarse aerosol population. For that reason, this factor is ascribed as the crustal factor, explaining 37.0% of the total variance. The second factor explains 28.1% of the total variance in the system, and can be identified as a marine factor, since it consists of high loadings of Na^+, Cl^-, Mg^{2+}, Br^- and high loadings of SO_4^{2-} and K^+ as well. Factor-3 is highly loaded in Ni and V and moderately loaded in Zn. Therefore, this factor is attributed to residual oil combustion, and explains 12.4% of the total variance. The fourth factor explains a further 10.3% of the variance and can be identified as photochemical sources, since it is highly loaded with NO_3^- and $C_2O_4^{2-}$.

TABLE 1a. Varimax rotated factor matrix and corresponding probable source type for the coarse aerosol data set

Variable	Factor1	Factor2	Factor3	Factor4	Communalities
Ti	**0.96**	0.13	0.17	0.16	0.99
Fe	**0.95**	0.16	0.19	0.13	0.99
Mn	**0.93**	0.11	0.12	0.14	0.98
Ca^{2+}	**0.84**	0.34	0.31	0.13	0.94
K	**0.82**	0.51	0.16	0.08	0.98
Zn	0.49	0.06	**0.62**	0.26	0.98
V	0.48	0.02	**0.80**	0.02	0.65
Ni	0.14	0.12	**0.93**	–0.03	0.80
Cr	0.16	-0.03	0.15	0.07	0.71
Cl^-	0.11	**0.99**	0.04	–0.08	0.99
Mg^{2+}	0.12	**0.97**	0.02	–0.05	0.98
Na^+	0.20	**0.97**	0.03	–0.03	0.99
Br^-	0.11	**0.96**	0.07	–0.08	0.96
SO_4^{2-}	0.37	**0.89**	0.12	0.16	0.96
$C_2O_4^{2-}$	0.26	0.04	0.09	**0.89**	0.68
NO_3^-	0.19	–0.15	–0.01	**0.91**	0.66
Eigen Value	6.7	5.1	2.2	1.9	
Variance, %	37.0	28.1	12.4	10.3	
Probable Source	Crustal	Marine	Residual Oil	Photochem.	

(B) Fine Particles: The variables of chemical species in the fine fraction may be explained on the basis of four common factors, elucidating 857% of the total system variance. The first factor has high loadings of SO_4^{2-}, NH_4^+, MS^-, $C_2O_4^{2-}$, Zn and moderate loading of K^+ and explains 28.1% of the total variance. Therefore, this factor can be ascribed to secondary aerosols as it has high loadings of sulfate, ammonium, methane-sulfonate and oxalate. Factor-2 consists of high loadings of Ti, Fe, Mn and Ca^{2+} and clarifies a further 28.1% of the total variance. Since Factor-2 is heavily affected by concentrations of Ti, Fe, Mn and Ca^{2+}, may be attributed to a crustal factor. The third factor is highly loaded in Na^+ and Mg^{2+} and explains 11.0% of the total variance in the system and may be ascribed to a marine factor. Factor-4 has high loadings of NO_3^-, V and Ni and accounts for 12.5% of the total variance of the system, and hence may be attributed to residual oil combustion.

Absolute principal factor analysis (APFA) was applied to quantify the contributions of the different sources to the concentrations of the measures species. For each coarse and fine aerosol component identified, the factor score was computed for each sample. Mass loadings for the samples were

TABLE 1b. Varimax rotated factor matrix and corresponding probable source type for the fine aerosol data set

Variable	Factor1	Factor2	Factor3	Factor4	Communalities
SO_4^{2-}	**0.96**	0.04	0.14	0.04	0.96
NH_4^+	**0.95**	–0.03	–0.01	0.16	0.95
$C_2O_4^{2-}$	**0.88**	0.11	0.28	0.20	0.88
MS^-	**0.80**	0.15	0.25	–0.11	0.72
K^+	0.62	0.04	0.10	0.24	0.52
Mg^{2+}	0.25	0.29	**0.85**	–0.04	0.73
Na^+	0.24	0.01	**0.90**	0.05	0.70
NO_3^-	0.06	0.04	0.21	**0.86**	0.43
V	0.47	0.18	–0.20	**0.77**	0.87
Ni	0.41	0.40	–0.21	**0.70**	0.86
Zn	0.79	0.22	0.03	0.29	0.70
Ti	0.09	**0.97**	0.04	0.03	0.98
Fe	0.09	**0.96**	0.08	0.07	0.99
Mn	0.17	**0.91**	0.03	0.13	0.86
Ca^{2+}	0.02	**0.87**	0.13	0.20	0.79
Cr	0.05	0.13	0.01	0.06	0.81
Eigen Value	4.8	4.8	1.9	2.1	
Variance, %	28.1	28.1	11.0	12.5	
Probable Source	Secondary	Crustal	Marine	Residual Oil	

then regressed on the AFCS (Absolute Factor Component Scores). The resultant regression coefficients were then applied to convert the daily absolute factors scores to estimate the mass contributions.

(A) Coarse Particulate Mass: The results in Figure 3a indicate estimated contributions from each of the identified sources in the coarse samples. Of the coarse fraction, the largest portion is attributable to the sea salt related source (59% of the coarse mass). In addition, a crustal component would explain 36% of the observed coarse fraction. Therefore, these naturally derived aerosol components explain 95% of coarse fraction. However, photochemistry and residual oil combustion contributes 3% and 2% of the detected coarse fraction.

(B) Fine Particulate Mass: The estimated contribution from identified sources is shown in Figure 3b. Secondary aerosol components make the largest contribution to the fine fraction (59%). Residual oil combustion related component explains a further 12.7% of the fine fraction. In addition, crust and sea salt explain 6.8% and 4.7% of measured fine fraction, respectively.

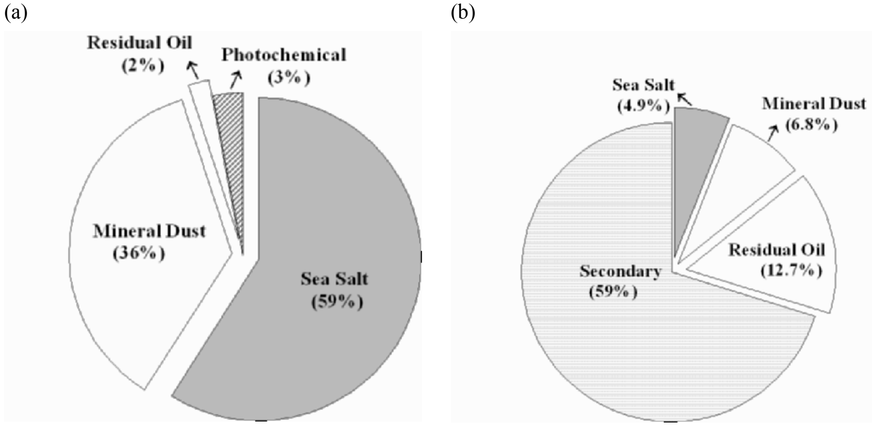

Figure 3. Estimated contribution from each source profile to particulate matter mass. (a) Coarse particulate matter mass and (b) Fine particulate matter mass

3.3. ORIGIN OF THE EXCEEDED PM_{10} LEVELS OF THE EUROPEAN DAILY LIMIT VALUE

Legislation of the PM_{10} limit values has been established by the European Commission for PM monitoring (EC/30/1999). The daily PM_{10} value has been limited to 50 $\mu g\ m^{-3}$, which may only be exceeded 35 days/year in 2005 (Phase I) and 7 days/year in 2010 (Phase II). A number of studies have focused on the origin of exceeded PM_{10} levels in the Western Mediterranean region (Artinano et al., 2001; Rodriguez et al., 2001). These studies have shown that exceedences of PM_{10} limit values may not always be caused by anthropogenic sources. This can be illustrated by using Spain as an example (various rural, urban and industrial sites, including the Canary Islands), where the studies indicated differences in PM_{10} chemical compositions (Rodriguez et al., 2001, 2002; Alastuey et al., 2005). These authors showed that PM_{10} concentrations are highly influenced by the occurrence of African dust. For example, more than half of the exceedences of PM_{10} at rural sites were attributed to the occurrence of African dust whereas approximately 20% of the exceedences of PM_{10} at urban and industrialized sites were originated from African dust transport. Therefore, at rural sites dust contributions might be considered to be an important contributor to the number of exceeded values of the EU daily limit value.

Figure 4 shows monthly arithmetic mean concentrations of PM_{10} at the Erdemli site. The seasonality of PM_{10} has been reported in rural, urban, and industrialized sites of the Western Mediterranean (Rodriguez et al., 2002) and the highest monthly PM levels are recorded in summer. In contrast, PM_{10} did not indicate a clear seasonal variability at Erdemli. However,

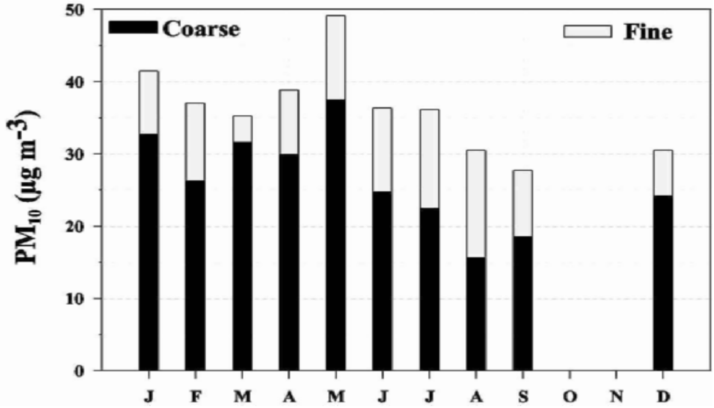

Figure 4. Monthly mean concentrations of PM$_{10}$

relative contributions of the fine fraction increased from winter to summer. For example, in August the relative contribution of fine fraction accounted for 50% of the PM$_{10}$ mass. This might be attributed to the enhancement of secondary aerosol (such as sulphate) generation during summer in the Mediterranean region (Kubilay et al., 2002; Koçak et al., 2004b).

At the Erdemli site annual PM$_{10}$ mass concentration is about 36.4 µg m^{-3} with high daily variability ranging between 1.5 and 326.0 µg m^{-3}. During the sampling period 28 events exceeded legislation of PM$_{10}$ limit values established by the European Commission for PM monitoring. In order to clarify the source (natural or anthropogenic) of the exceedences of the forthcoming EU daily limit values, air mass back trajectories, concentrations of Fe (Ti and nssCa^{2+}; indicator of crustal material), Na^{+} (indicator of sea spray), pollution indicators nssSO$_4^{2-}$ and NO$_3^{-}$ and TOMS aerosol absorbing index were used.

Figure 5a shows an example of the source apportionment of the PM$_{10}$ limit value due to Saharan air mass transport which occurred on the 6th of April 2002. On April 6th, the back trajectories at all four levels (see Figure 6a) indicate air mass flow arriving at Erdemli from North Africa. The TOMS image also shows an intense dust cloud over the North Africa and the northeastern Mediterranean (see Figure 6b). During this event the dust concentration was found to be around 85 µg m^{-3}. Dust contribution accounted for 78% of the PM$_{10}$ level while sea salt explained 12% of PM$_{10}$. In addition, nssSO$_4^{2-}$ and NO$_3^{-}$ together accounted for 7% of PM$_{10}$.

On the 17th of December 2001, PM$_{10}$ was found around 60 µg m^{-3} due to maritime air mass transport at 1000 hPa and 850 hPa. During this event sea salt concentrations were found to be high (47 µg m^{-3}) and the sea salt origin was also confirmed by the source apportionment analysis (see Figure 5b).

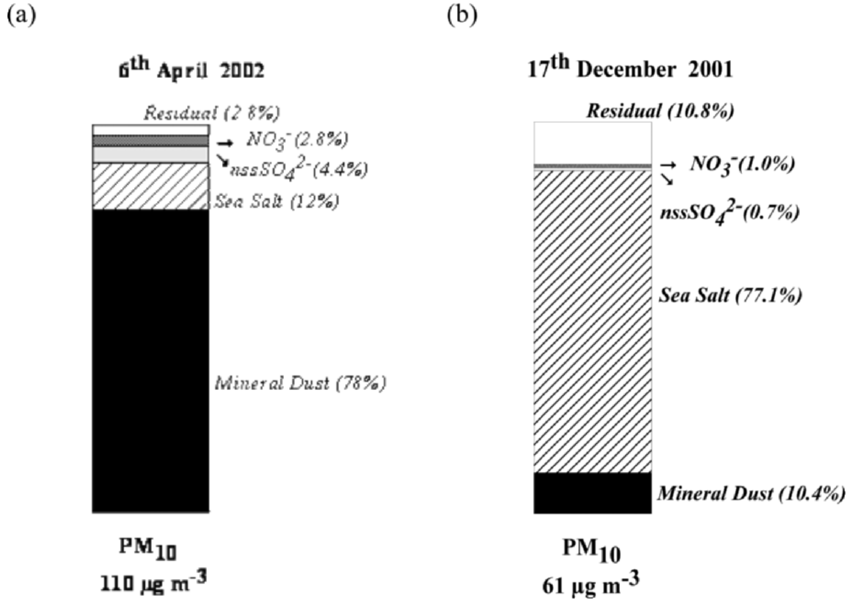

Figure 5. Source apportionment analysis for PM_{10} (a) during the Saharan dust event on the 6th of April 2002; (b) during the sea salt event on the 17th of December 2001

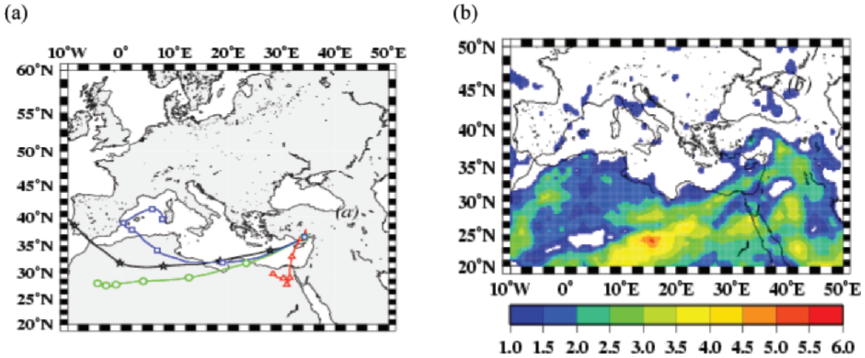

Figure 6. Saharan dust transport observed on 6th of April 2002 (a) Air mass back trajectories (b) TOMS Aerosol Absorbing Index

The source apportionment showed that sea salt accounted for 77.1% of the PM_{10} level while dust contribution explained for 10.4% of the PM_{10}. In addition, $nssSO_4^{2-}$ and NO_3^- together explained a small fraction (1.7%) of the PM_{10}.

3.4. AEROSOL IONIC BALANCE

Ion balance means the sum of the negative ions (anions) equals the sum of the positive ions (cations) when expressed as equivalents. An ion balance can be a useful tool to determine any possible parameters missing for the ionic balance. For this purpose, an ion balance was performed both in the coarse fine fractions of the aerosol particles. Plot of total cations equivalents against total anions equivalents for each size class are presented in Figures 7a and 7b, respectively. The slope of the regression line for coarse particles indicates value higher than unity (slope = 1.14, r = 0.97), which may be due to the existence of CO_3^{2-} in this size fraction which has not been measured using IC. In contrast, the slope of the regression line for the fine fraction is lower than unity (slope = 0.70, r = 0.97), which may be attributed to be presence of H^+ (not measured) in the aerosol samples. If this is the case, CO_3^{2-} is expected to associate with Ca^{2+} and H^+ is expected to react with SO_4^{2-} in the coarse and fine fractions, respectively (Figure 8a, b). A statistically significant correlation was found when Ca^{2+} concentrations were plotted against the anion deficit, defined as an excess of positive charge, indicating that CO_3^{2-} is most probably the missing anion in the coarse aerosol fraction. A significant correlation was also found between SO_4^{2-} and the cationic deficit in the fine fraction, that the cation deficit, defined as an excess of negative charge, is possibly due to H^+ associated with SO_4^{2-}.

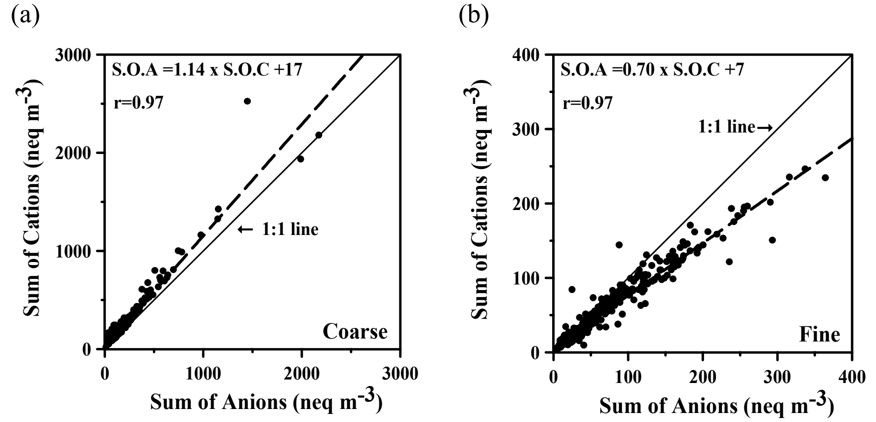

Figure 7. Sum of the anions *vs* sum of the cations: (a) Regression analysis in coarse samples, (b) Regression analysis in fine samples

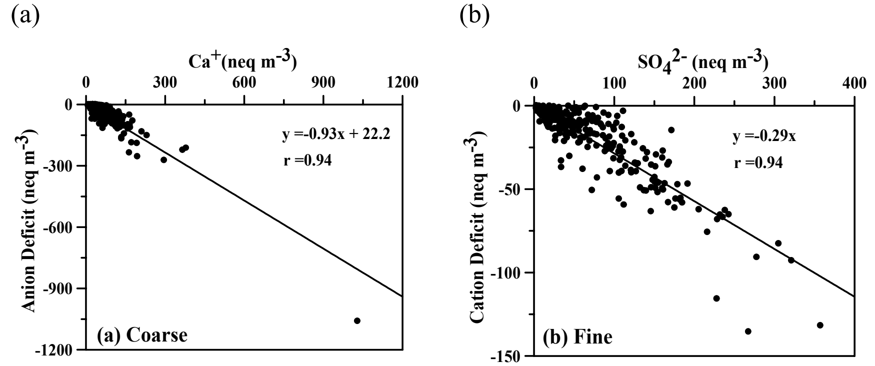

Figure 8. (a) Variation of anion deficit versus the Ca^{2+} concentrations in coarse samples, (b) Variation of cation deficit versus the SO_4^{2-} concentrations in fine samples.

4. Conclusions

$PM_{2.5-10}$, $PM_{2.5}$ and PM_{10} concentrations, factors controlling their levels and the origin and chemical composition of their exceedences have been identified at rural site located on the coast of the Eastern Mediterranean. From these findings the following conclusions may be made:

Annual mean concentrations of PM_{10} and $PM_{2.5}$ at Erdemli were 36.4 ± 27.8 μg m^{-3} 9.7 ± 5.9 μg m^{-3}, respectively, while concentrations indicated orders of magnitude change from day to day (PM_{10} = 2 to 326 μg m^{-3}; $PM_{2.5}$ = 0.5 to 28 μg m^{-3}). PM_{10} exhibited higher concentrations particularly during transition period due to mineral dust transported from North Africa and during winter owing to sea spray generation. $PM_{2.5}$ shows higher concentration mainly during summer as a result of an enhanced production of secondary aerosols.

PM_{10} mass is dominated by coarse fraction which accounts to about 75% of the total PM_{10} concentration. Crust (Fe, Ti, Mn, Ca), sea salt (Na^+, Cl^-, Mg^{2+}, Br^-) originated species and NO_3^- are associated mainly with coarse particles (>75%) whilst trace elements Cr and Ni and water soluble ions $nssSO_4^{2-}$, $C_2O_4^{2-}$, MS^- and NH_4^+ are primarily found in the fine fraction (>60%). V and Zn are found equally distributed between coarse and fine particles.

Investigation of the relationship between $nssSO_4^{2-}$ and NH_4^+ indicates that sulphate particles are not sufficiently neutralized by basic NH_4^+. Equivalent ratio ($NH_4^+/nssSO_4^{2-} = 0.68$) exhibits that about 70% of the $nssSO_4^{2-}$ is neutralized by NH_4^+. Excess-K/BC presents two distinct ratios for winter (0.066) and summer (0.366), indicating two contrasting BC sources in the area.

These ratios suggest that in the winter BC is mainly originated from fossil fuel burning whilst it is predominantly emitted from biomass burning in the summer.

Aerosol ionic balance analyses imply that coarse and fine particles show basic and acidic character. Basic and acidic character for coarse and fine fraction might be attributed to the presence of CO_3^{2-} and H^+ in the aerosols, respectively.

5. Acknowledgements

This study was funded in part by the Middle East Technical University (AFP-2001-07-01-01) and WMO (through special service agreements of 5.115/A/CNS and 18.637/A/CNS). The authors would like to thank the NASA/GSFC/TOMS group for the use of TOMS Aerosols Index data, and Emin Özsoy for making available the ECMWF trajectory analysis through collaboration with the Turkish State Meteorological Office. Mustafa Koçak benefited from the research fellowship of the International Atomic Energy Agency (TUR/0/006) and RICAMERE project.

6. References

Alastuey, A., Querol, X., Castillo, S., Escudero, M., Avila, A., Cuevas, E., Torres, C., Romero P. M., Exposito, F. and García, O., 2005, Characterisation of TSP and PM2.5 at Izaña and Sta. Cruz de Tenerife (Canary Islands, Spain) during a Saharan Dust Episode (July 2002), *Atmos. Environ.*, **39:** 4715-4728.

Andreae, M. O., 1983, Soot carbon and excess fine potassium: long-range transport of combustion derived aerosols, *Science* **220:** 1148-1151.

Artinano, B., Querol, X., Salvador, P., Rodriguez, S., Alonso, D.G. and Alastuey A., 2001, Assessment of airborne particulate levels in Spain in relation to the new EU-directive, *Atmos. Env.* **35:** 43-53.

Bardouki, H., Liakakou, H., Economou, C., Sciare, J., Smolik, J., Zdimal, V., Eleftheriadis, K., Lazaridis, M., Dye, C. and Mihalopoulos, N., 2003, Chemical composition of size resolved atmospheric aerosols in the eastern Mediterranean during summer and winter, *Atmos. Environ.* **37:** 195-208.

Borbely-Kiss, I., Koltay, E., Szabo, Gy., Bozo, L. and Tar, K., 1999, Composition and sources of urban and rural atmospheric aerosol in Eastern Hungary, *Journal of Aerosol Scence* **30:** 369–391.

IPCC, 2001, Climate Change 2001, Intergovernmental Panel on Climate Change, *Cambridge University Press*, London.

Jacobson, M. Z., 2001, Global direct radiative forcing due to multicomponent anthropogenic and natural aerosols, *J. Geophys. Res.* **106:** 1551-1568.

Kaufman, Y. Tanre, J. D. and Boucher, O., 2002, A satellite view of aerosols in the climate system, *Nature* **419:** 215-223.

Koçak M., Nimmo, M., Kubilay, N. and Herut, B., 2004a, Spatio-temporal aerosol trace metal concentrations and sources in the Leventine Basin of the Eastern Mediterranean, *Atmos. Environ.* **38:** 2133-2144.

Koçak, M., Kubilay, N. and Mihalopoulos, N., 2004b, Ionic composition of lower tropospheric aerosols at a Northeastern Mediterranean site: implications regarding sources and long-range transport, *Atmos. Environ.* **38:** 2067-2077.

Kubilay, N. and Saydam, C., 1995, Trace elements in atmospheric particulates over the Eastern Mediterranean: concentration, sources and temporal variability, *Atmos. Environ.* **29:** 2289-2300.

Kubilay, N., Koçak, M., Çokacar, T., Oğuz, T., Kouvarakis, G. and Mihalopoulos, N. 2002, Influence of Black Sea and local biogenic activity on the seasonal variation of aerosol sulfur species in the eastern Mediterranean atmosphere, *Global Biogeochemical Cycles* **16(4):** 1079, doi:10.1029/2002GB001880.

Ramanathan, V., Crutzen, P. J., Kiehl, J. T. and Rosenfeld, D., 2001, Aerosols, climate, and the hydrological cycle, *Science* **294:** 2119-2124.

Rodriguez, S., Querol, X., Alastuey. A., Kallos, G. and Kakaliagou, O., 2001, Saharan dust contributions to PM10 and TSP levels in Southern and Eastern Spain, *Atmos. Environ.* **35:** 2433-2447.

Rodriguez, S., Querol, X., Alastuey, A. and Plana, F., 2002, Sources and processes affecting levels and composition of atmospheric aerosol in the western Mediterranean, *J. Geophys. Res.* **107 (D24):** 4777, doi:10.1029/2001JD001488.

Sciare, J., Cachier, H., Oikonomou, K., Ausset, P., Sarda-Estève, R. and Mihalopoulos, N., 2003, Characterization of Carbonaceous Aerosols during the MINOS campaign in Crete, July-August 2001, *Atmos. Chem. Phys.* **3:** 1743-1757.

Vrekoussis, M., Liakakou, E., Koçak, M., Kubilay, N., Oikonomou, K., Sciare, J. and Mihalopoulos, N., 2005, Seasonal variability of optical properties of aerosols in the eastern Mediterranean, *Atmos. Environ.* **39:** 7083-7094.

Yang, F., He, K., Ye, B., Chen, X., Cha, L., Cadle, S. H., Chan, T. and Mulawa, P. A., 2005, One-year record of organic and elemental carbon in fine particles in downtown Beijing and Shanghai, *Atmos. Chem. Phys.* **5:** 217-241.